CHEMISTRY
A EUROPEAN JOURNAL

DOI: 10.1002/chem.200802334

# Size Selection During Crystallization of Oppositely Charged Nanoparticles

**Bartlomiej Kowalczyk,[a, b] Alexander M. Kalsin,[b] Rafal Orlik,[a, b, c] Kyle J. M. Bishop,[b] Alexander Z. Patashinskii,[a, b] Antoni Mitus,[c] and Bartosz A. Grzybowski*[a, b]**

Self-assembly of nanoscopic components into ordered "suprastructures" is a promising route to new types of nanomaterials with applications in catalysis,[1] optoelectronics,[2] and biological sensing,[3] to name just a few. We have recently shown that electrostatic interactions between oppositely charged nanoparticles (NPs, Figure 1a) can mediate self-assembly of large, three-dimensional crystals comprising up to tens of millions of NPs (Figure 1b).[4] These experiments were based on Au and/or Ag nanoparticles having similar average sizes (typically, $d^+ = d^- \approx 5.5$ nm) and varying degrees of polydispersity (from $\approx 5\%$ to 40%). Remarkably, such NPs crystallized from solution into a diamond (i.e., ZnS) lattice rather than NaCl or CsCl structures expected for "analogous" ($q^+/q^- \approx -1$, $d^+/d^- \approx 1$), ionic crystals. The major driving force in the formation of the low-packing-fraction diamond structure was the tendency of the next-nearest-neighbor, like charged particles to separate by at least twice the Debye screening length (few nm) and thereby to reduce the unfavorable electrostatic repulsions.[4a] These and other results,[4b,c,5] including the ability to control the charges of the NPs down to few percent,[6] suggest that charged NPs are unique building blocks (which we termed "nanoions"[4c]) from which one could build three-dimensional nanostructured materials of unusual modes of internal organization. To realize this vision, however, it should be possible to use "nanoions" of different sizes and charges and assemble them into various types of crystalline lattices. Although apparently simple in concept, the extension from like-sized to differently-sized particles is complicated by the tendency of the latter to aggregate into an amorphous phase. In this paper, we study such effects by varying the size distributions of the co-crystallizing NPs. We show that good-quality supracrystals form only when these distributions overlap to some degree. Remarkably, in such case, the crystals "select" only the NPs from the overlap region; other particles—even if their relative sizes are, in principle, suitable to fit into a binary crystal—form only an amorphous precipitate. Similarly, for non-overlapping distributions the particles do not crystallize at all (irrespective of the ratio of mean diameters $d^+/d$), but aggregate to form the amorphous phase exclusively. These size-selection effects are in sharp contrast to the results of nanoparticle crystallization on 2D supports in which the presence of the substrate and dramatic reduction of the solvent volume during assembly can force the NPs into multilayer, crystalline arrangements comprising particles of different sizes.[7] Monte-Carlo simulations and analyses based on lattice-invariants corroborate our experimental results and suggest that size-selection for charged particles is a thermodynamic rather

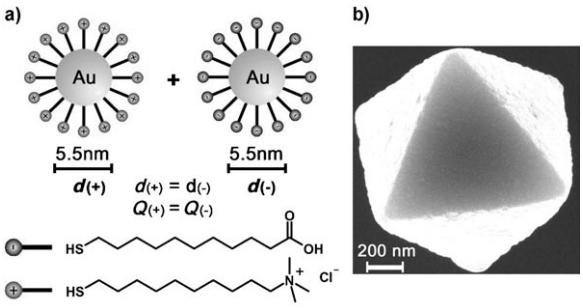


Figure 1. a) Scheme of the oppositely charged gold nanoparticles. Positively charged NPs are functionalized with *N,N,N*-trimethyl(11-mercaptoundecyl)ammonium chloride (TMA); negatively charged NPs are coated with a SAM of deprotonated mercaptoundecanoic acid (MUA). b) An SEM image of a supracrystal comprising $\approx 2.5$ million NPs.

[a] Dr. B. Kowalczyk, Dr. R. Orlik, Prof. Dr. A. Z. Patashinskii, Prof. Dr. B. A. Grzybowski
Department of Chemical Engineering, Northwestern University
2145 Sheridan Rd., Evanston, IL, 60208 (USA)
Fax: (+1) 847-491-3728
E-mail: grzybor@northwestern.edu

[b] Dr. B. Kowalczyk, Dr. A. M. Kalsin, Dr. R. Orlik, K. J. M. Bishop, Prof. Dr. A. Z. Patashinskii, Prof. Dr. B. A. Grzybowski
Department of Chemistry, Northwestern University
2145 Sheridan Rd., Evanston, IL, 60208 (USA)

[c] Dr. R. Orlik, Prof. Dr. A. Mitus
Institute of Physics, Wroclaw University of Technology
Wybrzeze Wyspianskiego 27, 50-370 Wroclaw (Poland)

Supporting information for this article is available on the WWW under http://dx.doi.org/10.1002/chem.200802334.

than kinetic phenomenon and can be attributed to entropic effects that "interfere" with the ordering of NP supracrystals.

We used gold and/or silver NPs, as described previously,[5] and made the average size of the metal cores in the various batches between 3 and 13.5 nm (typical standard deviations, $\sigma \approx 5$–$20\,\%$). The NPs were functionalized with self-assembled monolayers (SAMs)[8] of either positively charged *N*,*N*,*N*-trimethyl(11-mercaptoundecyl)ammonium chloride (TMA, $pK_a > 13$; from ProChimia Surfaces, Poland) or with negatively charged mercaptoundecanoic acid (MUA, $pK_a$ in the NP/SAM $\approx$ 6–8), with the pH of the latter adjusted to 11 to fully deprotonate the carboxylic groups. In all experiments, the binary NP solutions were electroneutral in terms of charges on the NPs (i.e., $\Sigma q_{NP(+)} + \Sigma q_{NP(+)} = 0$) and the crystals were grown from 1:1 *v*/*v* water/DMSO solutions, according to the procedure outlined in the Experimental Section.

The three typical outcomes of NP crystallization are illustrated in Figure 2. If the size distributions of the (+) and (−) NPs fully overlap (Figure 2a), the majority of NPs assemble into large, high-quality crystals that sediment from the solution. When the supernatant was decanted and the solid washed twice with acetonitrile, the crystals were analyzed in two ways. First, SEM images of the faces of individual crystals were taken: these faces were smooth, had few defects, and the particles within each crystal had low polydispersities ($< 5\,\%$ vs. $\sigma > 15$–$20\,\%$ for the initial (+) and (−) NP distributions). Second, when the statistics were taken over several crystals or when all crystals were redissolved in water and the sizes of the NPs were analyzed by TEM, the polydispersities were significantly larger ($\approx 15\,\%$). These observations indicate that although each supracrystal incorporates oppositely charged NPs of maximally matching/equal sizes, the average sizes of NPs within different crystals vary.

If the average sizes of (+) and (−) NPs are different, but the size distributions still overlap (Figure 2b), only the particles in the region of overlap crystallize, whereas others form amorphous precipitate. The crystals that grow are markedly smaller than in the case of fully overlapping distributions, and the crystal faces are rough, occasionally incorporating particles of mismatched sizes.

Finally, when the average NP sizes are markedly different and the distributions are not overlapping, no well-defined crystals are observed at all (save some small clusters with a semblance of ordered arrangement), and the particles aggregate into an amorphous precipitate (Figure 2c).

All of the above trends are also observed for NP sizes and types (e.g., AgTMA/AuMUA or AgMUA/AuTMA) other than those shown in Figure 2 and for pH in the range 10 to 12. For lower pH, the quality of crystals is systematically worse, likely as a result of the reduction in the magnitude of electrostatic forces and the introduction of additional interactions, such as hydrogen bonding.[9]

To explain the origin of the size selection, we performed a series of Monte Carlo (MC) simulations (theoretical details will be published separately), in which the interactions between particles *i* and *j* (charges $q_i$ and $q_j$, radii, $a_i$ and $a_j$, respectively) separated by a center-to-center distance $r_{ij}$ were expressed as a sum of screened electrostatic (ES), van der Waals (vdW), and hard sphere (HS) potentials in Equations (1)–(3):

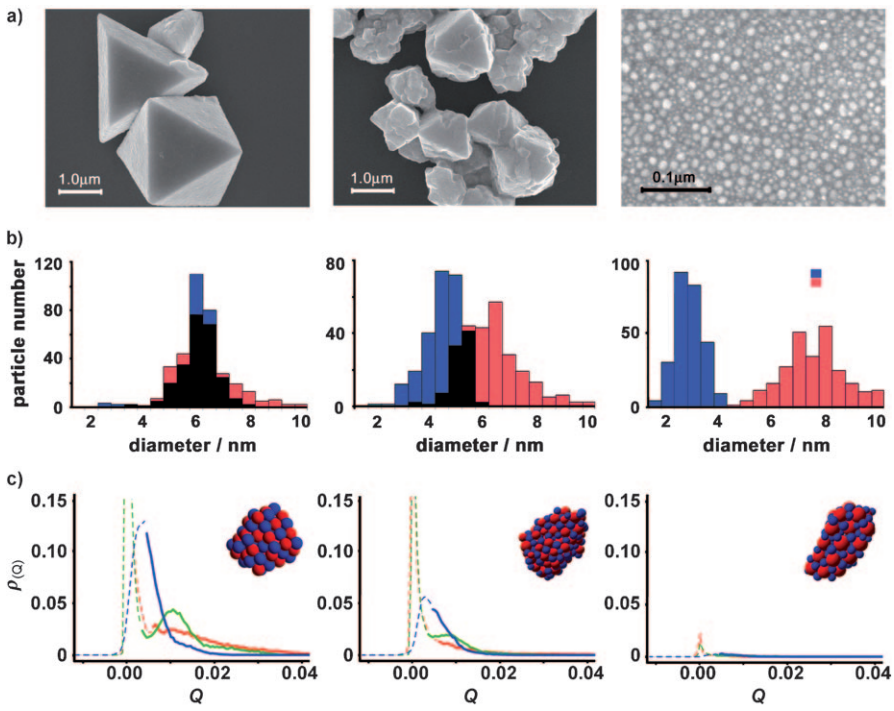


Figure 2. Size selection during crystallization of oppositely charged NPs. a) SEMs and b) histograms of NP size distributions. In all plots the blue histograms correspond to negatively charged AuMUA NPs, red histograms are for positively charged AuTMAs. The data shown is for typical NP batches; more monodisperse distributions give qualitatively similar results. The overlap regions are colored black. Statistics are based on the TEM measurements of 500 NPs from each batch. c) Normalized frequency distributions of invariants recognizing diamond lattice in the assemblies simulated by Monte Carlo. The local ordering is recognized as diamond if the invariants (see the Experimental and Supplementary Information for details) are: $Q_{4,4,8} > 0.00575$ (——), $Q_{4,6,10} > 0.00345$ (——), and $Q_{6,8,10} > 0.00430$ (——). Decaying invariant intensities (from the left to the right graph) reflect the fact that crystallinity of the assemblies decreases with decreasing degree of overlap between NP size-distributions (cf. graphs in b). Insets give illustrative zoom-outs of the assemblies (for clarity, only small subsets of 4096 NPs modeled in each MC run are shown).

  

$$U_{ES}(r_{ij}) = \frac{q_i q_j}{4\pi\varepsilon_0\varepsilon}\frac{\exp(\kappa(a_i+a_j))}{\varepsilon(1+\kappa a_1)(1+\kappa a_j)}\frac{\exp(-\kappa r_{ij})}{r_{ij}} \quad (1)$$

$$U_{vdW}(r_{ij}) = -\frac{a}{3}\left[\frac{a_i^c a_j^c}{r_{ij}^2-(a_i^c+a_j^c)^2}+\frac{a_i^c a_j^c}{r_{ij}^2-(a_i^c-a_j^c)^2} + \frac{1}{2}\ln\frac{r_{ij}^2-(a_i^c+a_j^c)^2}{r_{ij}^2-(a_i^c-a_j^c)^2}\right] \quad (2)$$

$$U_{HS}(r_{ij})\left\{\begin{array}{l}\infty\ r \le a_i+a_j\\ 0\ \ r > a_i+a_j\end{array}\right\} \quad (3)$$

In the electrostatic potential, $\kappa^{-1} \equiv (\varepsilon_0\varepsilon k_B T/2ce^2)^{1/2}$ is the Debye screening length, for which $\varepsilon_0$ is the permittivity of vacuum, $\varepsilon$ is the dielectric constant of the solvent (here, $\varepsilon = 60$ corresponding to a 1:1 mixture of DMSO and water), $e$ is the elementary charge, $c$ is the (monovalent) salt concentration (typically, $c \approx 1$ mM), and $k_B T$ is the thermal energy. In the van der Waals potential, $A = 4\times10^{-19}$ J is the Hamaker constant for the NP cores (i.e., gold across water), and $a^c = a - \delta$ is the radius of the NP's metal core, in which $\delta \approx 1.5$ nm is the thickness of the self-assembled monolayer (SAM) covering the NPs. In all simulations, it was assumed that each particle had constant surface charge density $\sigma = \pm 0.015\ \mathrm{C\,m^{-2}}$ (in agreement with experimental zeta potential measurements), such that the NP charge $q$ was given by $q = 4\pi a^2\sigma$. The screening length was set to 9 nm, corresponding to the experimental conditions (i.e., $T = 65\,^\circ$C, $c =$ 1 mM, $\varepsilon = 60$). In all simulations, the particle size distributions were taken from experiments.

As illustrated in Figure 2d, these simulations reproduced the experimental trends qualitatively, with overlapping distributions leading to crystalline aggregates and non-overlapping distributions, to non-crystalline NP arrangements. We make two important comments regarding these results. First, the fact that an inherently equilibrium MC method gives agreement with experiment suggests that size-selection is under thermodynamic control and is not a kinetic phenomenon (e.g., flocculation of the aggregates comprising size-mismatched nanoparticles). Second, close analysis of the modeled assemblies by using lattice invariants recognizing/classifying local NP packing (invariants need to be used since the simulated assemblies of polydisperse NPs are never perfect crystals with long-range order; see Experimental and Supporting Information) shows that the proportion of crystalline phases in the aggregated structures decreases rapidly with increasing NP size difference, and non-overlapping NP distributions do not even form small, ordered clusters. Colloquially speaking, non-overlapping distributions do want to aggregate, but they have too many possible lattices to evolve into. Since the screened electrostatic forces are short-ranged, there is little energetic preference between ordered and disordered aggregates, and so the formation of high-quality crystals in entropically disfavored.

The conclusion from both the experiments and the simulations is therefore a negative one - namely, that 3D crystals cannot be easily grown from charged nanoparticles of different average sizes and finite polydispersities. In principle, entropic limitations could be overcome if the polydispersities of the NPs were significantly reduced. Still, even if the NP size distributions were delta-like functions, one should remember that not only the diameters but also the charges of the NPs should match to form a unique, regular lattice. For instance, assuming we were able to prepare monodisperse "nanoions" of relative sizes $d^+/d^- \approx 0.6$ for which a NaCl structure is expected for monovalent ions, the charges on the NPs would not be $q^+/q^- \approx -1$ but would instead scale as the square of the NP diameters, $q^+/q^- \approx -0.36$. Consequently, the unit cell of the NaCl lattice would not be electroneutral in terms of NP charge, and the supracrystals might still not form (note that incorporation of additional counterions to ensure electroneutrality is entropically unfavorable).

The way around this conundrum might be to adjust the sizes and the charges of the NPs *simultaneously*, the latter with the help of mixed SAMs. Although methods for controlling both of these variables are now available,[6,10] synthesis of "nanoionic" crystals will certainly challenge our ability to manipulate matter at the nanoscale. In the meantime, lattice invariants introduced in this work provide a new, general-purpose mathematical tool with which to study and quantify local ordering in assemblies of polydisperse objects.

## Experimental Section

**NP synthesis and crystal growth**: Gold and silver nanoparticles were synthesized and functionalized with SAMs of *N,N,N*-trimethyl(11-mercaptoundecyl)-ammonium chloride (TMA, ProChimia Poland) or mercaptoundecanoic acid (MUA, ProChimia) as previously described in Ref. [4]. Solution of MUA NPs (typically $c = 2$–5 mM, in terms of metal atoms) was deprotonated at pH 11 with tetramethylammonium hydroxide (0.2 M) and titrated with a solution of similar concentration of TMA NPs. As was shown in Refs. [5] and [6], the titrated solutions remained stable until precipitating rapidly at the point when the charges of the nanoparticles were neutralized (i.e., when $\Sigma q_{NP(+)} + \Sigma q_{NP(+)} = 0$). The electroneutral nanoparticle precipitate thus obtained was washed several times with copious amounts of water to remove salts, redissolved in deionized water at 60–65 °C and finally microfiltered to give a stable (for weeks) 0.5–4 mM solution containing oppositely charged NPs. Immediately prior to use, the pH of the solution was adjusted to a desired value (optimally, pH $\approx$10–11; by dropwise addition of 0.2 M $NMe_4OH$). Crystals were grown by mixing the electroneutral solution with DMSO in 1:1 v/v ratio and slowly ($\approx$16–24 hrs) evaporating water at 65 °C. DMSO was removed and crystals washed twice with acetonitrile. Crystals stored in acetonitrile solution and were stable for at least several months.

**Lattice invariants and structure classification**: Assemblies of polydisperse NPs that exhibit only local ordering can be characterized by lattice invariants, which are mathematical constructs based on various spherical harmonics. In general, a lattice invariant is a function $Q$ that depends on the positions of each of the $N$ nearest neighbors, that is, $Q \equiv Q(\{\vec{r}_j : 1 \le j \le N\})$ in which $\vec{r}_j$ denotes a vector between central atom and its $j$ nearest neighbor. Here, we used the so-called third-order structural invariants defined in Equation 4:

$$Q_{l_1 l_2 l_3} = \sum_{m_1 m_2 m_3}\begin{pmatrix} l_1 l_2 l_3 \\ m_1 m_2 m_3\end{pmatrix} Q_{l_1 m_1} Q_{l_2 m_2} Q_{l_3 m_3} \quad (4)$$

In which (…) stands for the Wigner 3j symbol, $Q_{l_1 m_1}$ denotes a linear combination of spherical harmonics seen in Equation (5):

$$Y(\theta,\varphi) : Q_{lm} = \frac{1}{N}\sum_{j=1}^{N} Y_{lm}(\theta_j,\varphi_j) \quad (5)$$

In which $(\theta,\varphi)$ are polar and azimuthal angles, respectively. The important properties of $Q_{l_1 l_2 l_3}$ are that a) it is independent of the coordinate system (hence, an "invariant") and b) assumes different values for different lattice types.

In the context of analysis/classification of NP assemblies, the key issue is then to find invariants that not only recognize, but also differentiate between different possible lattices. This was done by performing an exhaustive search of all invariants for which the values of the $l$ indices were even and varied between 4 and 10 (corresponding to the number of nearest neighbors in typical lattices) and applying these invariants to common lattices (diamond, simple cubic, fcc, bcc, hcp, icosahedral) with a certain degree of fluctuation around the equilibrium positions added. The fluctuations effectively accounted for the imperfections of the lattices made of polydisperse NPs and gave characteristic "signatures," $\rho_\Gamma(Q_{l_1 l_2 l_3})$, of each lattice, $\Gamma$, assuming it is being described by invariant $Q_{l_1 l_2 l_3}$. The maximally selective invariants for each lattice were then identified by calculating "overlap" integrals $E_{xy}$ for each invariant against all possible lattice pairs, $\Gamma_x$, $\Gamma_y$: $E_{xy} = \int \min(\rho_{\Gamma x}(Q_{l_1 l_2 l_3}), \rho_{\Gamma y}(Q_{l_1 l_2 l_3}))dQ_{l_1 l_2 l_3}$. Mathematical details of these operations are discussed in detail in the Supporting Information.

## Acknowledgements

This work has been supported by the Sloan Fellowship and the Dreyfus Teacher-Scholar Award (to B.A.G.)

**Keywords:** crystals · electrostatic interactions · lattice invariants · nanoparticles · self-assembly

[1] J. Grunes, J. Zhu, E. A. Anderson, G. A. Somorjai, *J. Phys. Chem. B* **2002**, *106*, 11463.
[2] S. A. Maier, P. G. Kik, H. A. Atwater, S. Meltzer, E. Harel, B. E. Koel, A. A. G. Requicha, *Nat. Mater.* **2003**, *2*, 229.
[3] M. Zayats, A. B. Kharitonov, S. P. Pogorelova, O. Lioubashevski, E. Katz, I. Willner, *J. Am. Chem. Soc.* **2003**, *125*, 16006.
[4] a) A. M. Kalsin, M. Fialkowski, M. Paszewski, S. K. Smoukov, K. J. M. Bishop, B. A. Grzybowski, *Science* **2006**, *312*, 420; b) A. M. Kalsin, B. A. Grzybowski, *Nano Lett.* **2007**, *7*, 1018; c) K. J. M. Bishop, B. A. Grzybowski, *ChemPhysChem* **2007**, *8*, 2171.
[5] A. M. Kalsin, B. Kowalczyk, S. K. Smoukov, R. Klajn, B. A. Grzybowski, *J. Am. Chem. Soc.* **2006**, *128*, 15046.
[6] A. M. Kalsin, B. Kowalczyk, P. Wesson, M. Paszewski, B. A. Grzybowski, *J. Am. Chem. Soc.* **2007**, *129*, 6664.
[7] a) K. P. Velikov, C. G. Christova, R. P. A. Dullens, A. van Blaaderen, *Science* **2002**, *296*, 106; b) M. E. Leunissen, C. G. Christova, A.-P. Hynninen, C. P. Royall, A. I. Campbell, A. Imhof, M. Dijkstra, R. van Roij, A. van Blaaderen, *Nature* **2005**, *437*, 235; c) A. Yethiraj, A. van Blaaderen, *Nature* **2003**, *421*, 513; d) A.-P. Hynninen, C. G. Christova, R. van Roij, A. van Blaaderen, M. Dijkstra, *Phys. Rev. Lett.* **2006**, *96*, 138308.
[8] D. Witt, R. Klajn, P. Barski, B. A. Grzybowski, *Curr. Org. Chem.* **2004**, *8*, 1763.
[9] L. Sun, G. Wei, Y. Song, L. Wang, C. Guo, Y. Sun, Z. Li, *Chem. Lett.* **2007**, *36*, 610.
[10] J. Park, J. Joo, S. G. Kwoon, Y. Yang, T. Hyeon, *Angew. Chem.* **2007**, *119*, 4714; *Angew. Chem. Int. Ed.* **2007**, *46*, 4630.

Received: November 10, 2008
Published online: January 13, 2009

  